Monte Carlo study of the droplet formation-dissolution transition on different two-dimensional lattices

A. Nußbaumer, E. Bittner, and W. Janke
Institut für Theoretische Physik and Centre for Theoretical Sciences (NTZ), Universität Leipzig, Postfach 100 920, D-04009 Leipzig, Germany

(Received 19 September 2007; revised manuscript received 21 December 2007; published 14 April 2008)

In 2003 Biskup *et al.* [Commun. Math. Phys. **242**, 137 (2003)] gave a rigorous proof for the behavior of equilibrium droplets in the two-dimensional (2D) spin-1/2 Ising model (or, equivalently, a lattice gas of particles) on a finite square lattice of volume V with a given excess $\delta M \equiv M - M_0$ of magnetization compared to the spontaneous magnetization $M_0 = m_0 V$. By identifying a dimensionless parameter $\Delta(\delta M)$ and a universal constant Δ_c, they showed in the limit of large system sizes that for $\Delta < \Delta_c$ the excess is absorbed in the background ("evaporated" system), while for $\Delta > \Delta_c$ a droplet of the minority phase occurs ("condensed" system). By minimizing the free energy of the system, they derived an explicit formula for the fraction $\lambda(\Delta)$ of excess magnetization forming the droplet. To check the applicability of the asymptotic analytical results to much smaller, practically accessible, system sizes, we performed several Monte Carlo simulations of the 2D Ising model with nearest-neighbor couplings on a square lattice at fixed magnetization M. Thereby, we measured the largest minority droplet, corresponding to the condensed phase in the lattice-gas interpretation, at various system sizes ($L = 40, 80, \ldots, 640$). With analytical values for the spontaneous magnetization density m_0, the susceptibility χ, and the Wulff interfacial free energy density τ_W for the infinite system, we were able to determine λ numerically in very good agreement with the theoretical prediction. Furthermore, we did simulations for the spin-1/2 Ising model on a triangular lattice and with next-nearest-neighbor couplings on a square lattice. Again finding a very good agreement with the analytic formula, we demonstrate the universal aspects of the theory with respect to the underlying lattice and type of interaction. For the case of the next-nearest-neighbor model, where τ_W is unknown analytically, we present different methods to obtain it numerically by fitting to the distribution of the magnetization density $P(m)$.

DOI: 10.1103/PhysRevE.77.041109 PACS number(s): 05.70.Fh, 02.70.Uu, 75.10.Hk

I. INTRODUCTION

The formation and dissolution of equilibrium droplets at a first-order phase transition is one of the long-standing problems in statistical mechanics [1]. Quantities of particular interest are the size and free energy of a "critical droplet" that needs to be formed before the decay of the metastable state via homogeneous nucleation can start. For large but finite systems, this is signaled by a cusp in the probability density of the order parameter ϕ toward the phase-coexistence region as depicted in Figs. 1 and 2 for the example of the two-dimensional (2D) Ising model, where $\phi = m$ is the magnetization. This cusp is often termed the evaporation-condensation "transition point" since it separates an "evaporated" phase with many very small bubbles of the "wrong" phase around the peak at ϕ_0 from the "condensed" phase, in which a large droplet has formed; for configuration snapshots see Fig. 3. The droplet eventually grows further toward $\phi = 0$ until it percolates the finite system in another droplet-strip "transition." The latter transition is indicated in the 2D Ising model by the cusp at the beginning of the flat two-phase region around $m = 0$ (see Fig. 1).

Following early work on the crystallization of hard spheres [2] and the general droplet picture [1], first numerical studies of the evaporation-condensation transition date back to the beginning of the 1980s [3–5]. Recently this problem was taken up again by Neuhaus and Hager [6], who discussed it with emphasis on possible Gibbs-Thomson and Tolman corrections. This stimulated further new theoretical [7–9] and numerical [10–13] work.

Here, we follow the exposition of Biskup *et al.* [7,8], who present their results both in a phenomenological liquid-vapor (or solid-gas) picture and also explicitly in terms of the simple Ising (lattice-gas) model. The distinguishing feature of their work is the formulation of a proper equilibrium theory which does not need to explicitly involve correction effects like those of Gibbs-Thomson or Tolman [14] as was done in earlier work [15–17]. We consider this feature as one of the main merits of their formulation, which can be shown

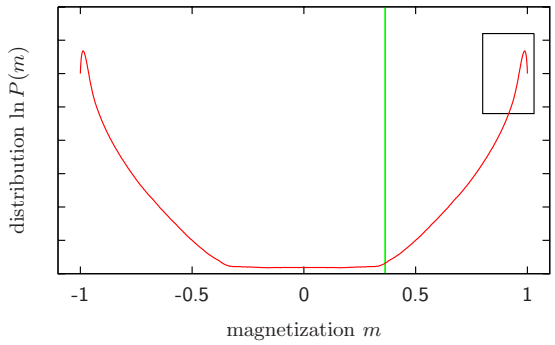

FIG. 1. (Color online) Schematic plot of the probability density $P(m)$ of the magnetization in logarithmic form. The marked box indicates the position of the cutout displayed in Fig. 2. The vertical (green) line indicates the droplet-strip transition point for positive magnetization $m > 0$, the use of which will be explained later on in Sec. III C.

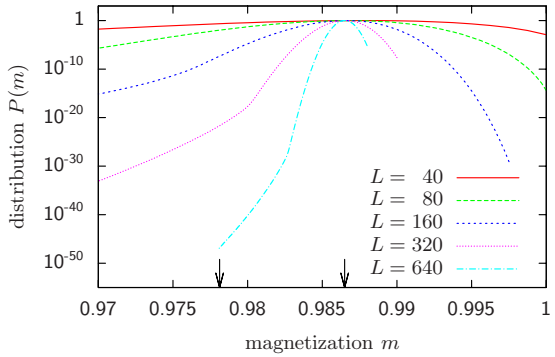

FIG. 2. (Color online) Probability density of the magnetization for the 2D Ising model around its right peak for different system sizes L at the temperature $T=1.5$. The cusp indicates the evaporation-condensation transition region. On the right side of the cusp (evaporated system), a Gaussian peak is clearly visible, while on the left side (condensed system), a stretched exponential behavior can be seen. The two arrows on the x axis indicate for $L=640$ the range of data points shown in Fig. 14 below.

to be equivalent (at least in leading order) to the earlier, less rigorous, treatment in [6].

The price one has to pay, however, is a rather intricate rescaling of the original problem, which in numerical work requires great care with details. To set the theoretical grounds for our Monte Carlo simulation study and in particular to develop intuition for the final representation of our results in Figs. 14–17 below, we therefore start first with a brief summary of the Biskup *et al.* [7,8] theory. In order to do so, we restrict ourselves to the special case of the 2D Ising model with Hamiltonian

$$\mathcal{H} = -J\sum_{\langle i,j\rangle} s_i s_j, \tag{1}$$

where $s_i = \pm 1$ and $\langle i,j\rangle$ denotes a (next-)nearest-neighbor pair. If a down spin ($s_i=-1$) is treated as a particle and an up spin ($s_i=+1$) as a vacancy, the system can be interpreted as a lattice gas of atoms.

II. THEORY

In this section we summarize the rigorous considerations of Biskup *et al.* [8] for the case of the 2D Ising model on a square lattice with nearest-neighbor interactions. While their proofs refer for technical reasons to this case only, the main line of arguments applies to other situations as well.

We imagine the following situation: an *unconstrained*[1] Ising system of size $V=L\times L$ in the low-temperature phase at the inverse temperature $\beta \equiv J/k_B T > \beta_c$. If the majority of spins is positive ($s_i=1$), i.e., the system is in the phase with positive magnetization, then, due to thermal fluctuations, there are always some overturned spins pointing in the opposite direction and the total magnetization $M=\sum_{i=1}^{V} s_i = m_0 V$. Here, $m_0=m_0(\beta)>0$ denotes the infinite-volume equilibrium

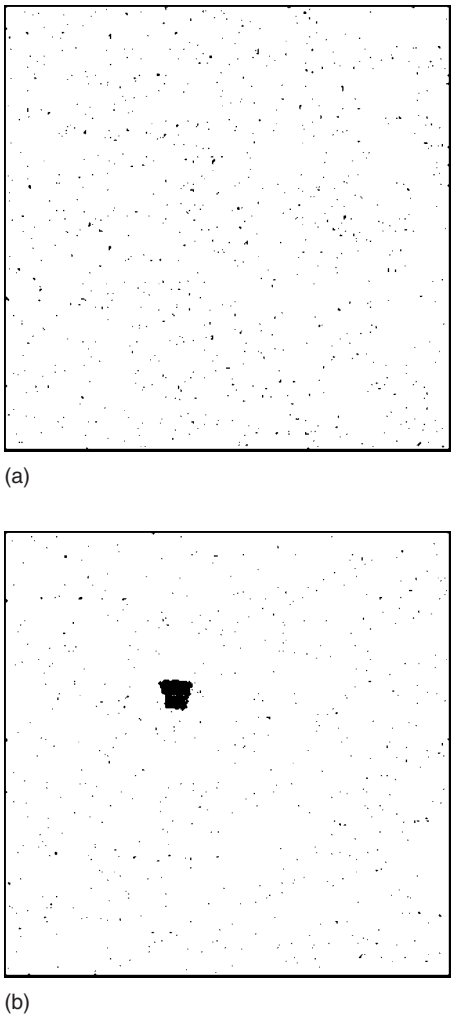

FIG. 3. Two snapshots of a 320×320 Ising system at $T=1.5$ and the same value of the magnetization $m=0.9801$ chosen to be in the vicinity of the evaporation-condensation point. (a) Evaporated system; a large number of very small excitations (bubbles) exist (1–4 spins) and the largest cluster consists of five connected spins. (b) Condensed system; a single large droplet with volume 400 spins that has absorbed a large amount of the small bubbles.

magnetization (spontaneous magnetization) as, e.g., calculated analytically by Onsager and Yang for the square lattice with nearest-neighbor interactions (see Sec. III).

Now, if some volume v_L of the systems is inverted,[2] then the magnetization of this *constrained* system is

$$M_L = m_0(V - v_L) - m_0 v_L. \tag{2}$$

For an illustration see Fig. 4. It is important to note that here we assumed the inverted volume v_L to have the magnetization $-m_0$, which is satisfied to a high degree for a large homogeneous system because of the erratic thermal fluctuations. Furthermore, the volume v_L must be chosen appropriately in order to be compatible with the magnetization M_L,

[1] Later on we will mostly consider constrained systems, i.e., systems where the magnetization is fixed.

[2] Inversion of spins means the operation $s_i \to -s_i$ for *all* spins in the volume v_L.

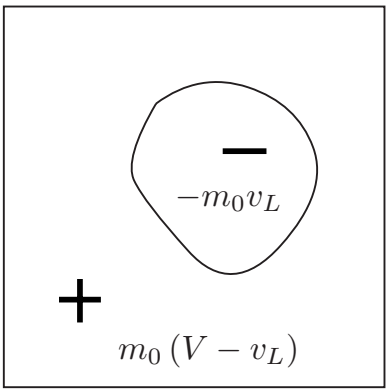

FIG. 4. Ising system of size V with a minority droplet of volume v_L of negative magnetization surrounded by the background volume $(V-v_L)$ of positive magnetization, shown in the extreme case where the total excess in magnetization is concentrated in the droplet, i.e., $v_d=v_L$.

which is an even integer value. Given the fact that m_0 is not an integer number, then the same must hold for v_L. In the asymptotic limit of large systems where the volume occupied by a single spin gets arbitrarily small compared to that of the whole system, possible ambiguities are removed.

Now, the difference (excess) from the original, unconstrained system with magnetization $M_0=m_0V$ is

$$\delta M_L = M_L - M_0 = -2v_L m_0. \tag{3}$$

The factor 2 is due to the definition of the Ising spins, having a value ± 1. The interpretation of this formula is as follows: a system that has a difference in the magnetization of δM_L from that of an unconstrained Ising system has a volume v_L of inverted spins.[3] Biskup *et al.* show that for a given magnetization M_L the total volume of inverted spins v_L can be (in the thermodynamic limit of large systems) decomposed into two parts, local fluctuations with total volume v_f and a single large connected droplet with volume v_d, since there exist no droplets of intermediate size [8]. For the total volume of inverted spins $v_L=v_f+v_d$ holds.

Now, the free energy can be decomposed according to the two contributions. For the droplet it is written as

$$F_d = \tau_W \sqrt{v_d}, \tag{4}$$

where τ_W is the interfacial free energy per unit volume of an ideally shaped droplet, also known as the free energy of a droplet of Wulff shape [18]. The contribution of the fluctuations is derived in the following manner. Of the volume V of the whole system v_d is already occupied by the single large droplet. The rest of the system has an unconstrained magnetization of $M_0^f=(V-v_d)m_0$. If some volume v_f of the remaining spins is inverted, then the magnetization is

$$M_f = (V - v_d - v_f)m_0 - m_0 v_f. \tag{5}$$

Then the difference δM_f from the unconstrained magnetization M_0^f is

$$\delta M_f = M_f - M_0^f = -2m_0 v_f. \tag{6}$$

The contribution to the free energy due to these fluctuations can be written as

$$F_f = \frac{(M_f - M_0^f)^2}{2\chi V} = \frac{2m_0^2 v_f^2}{\chi V}, \tag{7}$$

where $\chi=\chi(\beta)=\beta V[\langle m^2\rangle-\langle m\rangle^2]$ is the susceptibility in the thermodynamic limit.

Now, the excess magnetization δM_d of the droplet compared to the total excess magnetization δM_L is defined as

$$\lambda = \frac{\delta M_d}{\delta M_L} \quad \text{or} \quad \delta M_d = \lambda\, \delta M_L. \tag{8}$$

Using Eq. (3), which connects δM_L and v_L, the excess magnetization of the droplet can be written as $\delta M_d=-2v_d m_0$ and the total excess magnetization as $\delta M_L=-2v_L m_0$. Therefore, λ can also be presented in terms of the inverted volume as

$$\lambda = \frac{v_d}{v_L} \quad \text{or} \quad v_d = \lambda v_L. \tag{9}$$

Hence, v_f can be written as

$$v_f = v_L - v_d = v_L\left(1 - \frac{v_d}{v_L}\right) = v_L(1-\lambda). \tag{10}$$

Using this relation, the total free energy $F=F_d+F_f$ is

$$F = \tau_W \sqrt{v_d} + \frac{2m_0^2 v_f^2}{\chi V} \tag{11}$$

$$= \tau_W \sqrt{\lambda v_L} + \frac{2m_0^2}{\chi V} v_L^2 (1-\lambda)^2, \tag{12}$$

or, in the form of Biskup *et al.*,

$$F(\lambda) = \tau_W \sqrt{v_L}\, \phi_\Delta(\lambda) \tag{13}$$

with

$$\phi_\Delta(\lambda) = \sqrt{\lambda} + \Delta(1-\lambda)^2 \tag{14}$$

and

$$\Delta = \frac{2m_0^2 v_L^2}{\chi V \tau_W \sqrt{v_L}} = \frac{2m_0^2 v_L^{3/2}}{\chi V \tau_W}. \tag{15}$$

Now, if the magnetization is fixed to some value, then the total volume of overturned spins is also fixed and using Eq. (2) we have

$$v_L = \frac{1}{2}\left(V - \frac{M_L}{m_0}\right). \tag{16}$$

As m_0, χ, and τ_W are constants, the only varying quantity in Eq. (13) is the relative volume of the droplet, λ. A fully

[3]Here, one has to be careful in which range Eq. (3) is valid. The idea is to have a large homogeneous system where any macroscopic part has the magnetization m_0. Problems arise if the formula is interpreted on a microscopic level. For any finite system, only an equation of the form $M=m_{\mathrm{bg}}(V-v_d)+m_d v_d$ is valid, where m_{bg} is the actual magnetization in the background and m_d is the actual magnetization in the droplet.

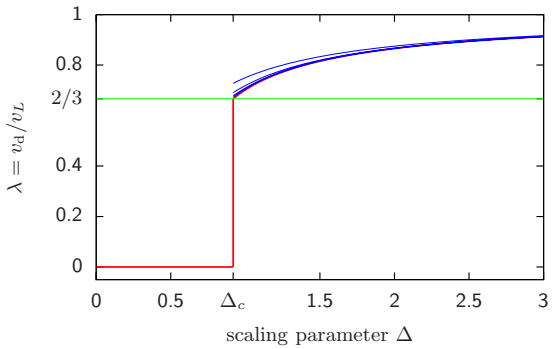

FIG. 5. (Color online) Fraction of the excess magnetization in the largest droplet, λ, in dependence on the scaling parameter Δ. For $\Delta<\Delta_c$ there is no largest droplet, only fluctuations. At $\Delta=\Delta_c$ a droplet is formed, containing 2/3 of the total excess. In the case $\Delta>\Delta_c$ the fraction of the excess is given by Eq. (21). The (blue) lines approaching λ for $\Delta>\Delta_c$ are the Taylor series of Eq. (21) up to order 4 around $\Delta=\infty$ that have the form $\lambda=1-1/4\Delta-1/32\Delta^2-5/512\Delta^3-1/256\Delta^4+\cdots$.

equilibrated thermodynamic system always stays in the minimum of the free energy. Therefore, the physical λ_Δ, i.e., the optimal partition of overturned volume between the droplet and the fluctuations, minimizes F in the range $\lambda\in[0,1]$. Consequently, the solution of this problem either is given by $\partial\phi_\Delta/\partial\lambda=0$, which is

$$\frac{1}{2\sqrt{\lambda}}-2\Delta(1-\lambda)=0, \tag{17}$$

or is one of the boundary values 0,1. The solution of Eq. (17) shows that for $\Delta<\Delta_c$ the correct solution is $\lambda=0$, i.e., pure fluctuations and no droplet at all. The point Δ_c it given by the condition $\phi_{\Delta_c}(0)=\phi_{\Delta_c}(\lambda_c)$, which is $\Delta_c=\sqrt{\lambda_c}+\Delta_c(1-\lambda_c)^2$, or

$$\Delta_c=\frac{1}{\sqrt{\lambda_c}(2-\lambda_c)}. \tag{18}$$

This can be substituted into Eq. (17) resulting in $1/2\sqrt{\lambda_c}-2(1-\lambda_c)/\sqrt{\lambda_c}(2-\lambda_c)=0$ or

$$\lambda_c=\frac{2}{3}. \tag{19}$$

Inserting this value into Eq. (18) gives

$$\Delta_c=\frac{3}{4}\sqrt{\frac{3}{2}}=0.918\,558\ldots. \tag{20}$$

For $\Delta>\Delta_c$ the solution is

$$\lambda=\frac{4}{3}\cos^2\left(\frac{\pi-\cos^{-1}(3\sqrt{3}/8\Delta)}{3}\right). \tag{21}$$

These results give rise to the following physical picture. For fixed magnetization $M_L\approx M_0$, where $\Delta(M_L)<\Delta_c$, the system contains no droplet; only fluctuations are present. At some value M_c with $\Delta(M_c)=\Delta_c$ two states coexist, the state of pure fluctuations and a mixed state composed of a droplet that absorbs 2/3 of the fluctuations and the remaining 1/3 of the fluctuations. For smaller magnetization, i.e., $\Delta(M_L)>\Delta_c$, the droplet grows and thereby absorbs more and more of the background fluctuations. The predicted behavior of $\lambda=\lambda(\Delta)$ is shown in Fig. 5.

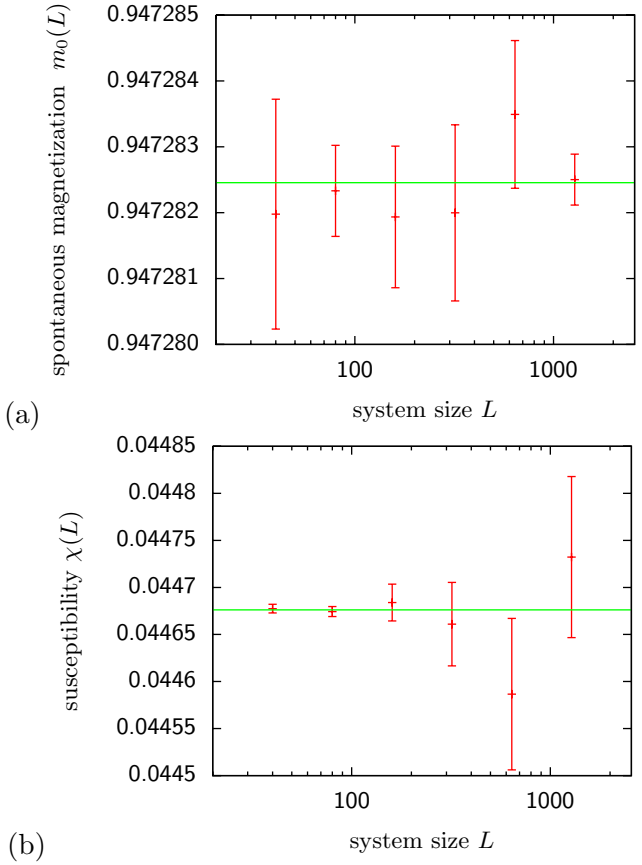

FIG. 6. (Color online) The horizontal (green) line marks the mean of (a) the spontaneous magnetization $m_0(L)$ and (b) the magnetic susceptibility $\chi(L)$ for system sizes $L=40,80,\ldots,1280$ at $T=4.0$ of a NNN Ising model. Its value gives an estimate for m_0 and χ at $L\to\infty$. Here, we read off the values $m_0=0.947\,2825(2)$ and $\chi=0.044\,676(2)$.

III. SETUP

In this work we wanted to answer two questions. On the one hand, we wanted to test for which system sizes the theoretical results presented in the last section start to yield a good description of the data for the standard 2D Ising model. On the other hand, we wanted to check the universal aspects of the theory by using different lattice models, namely, the triangular nearest-neighbor (NN) lattice and the next-nearest neighbor (NNN) square lattice. In order to do so, λ, the fraction of the excess of magnetization in the largest droplet defined in Eq. (9), has to be measured in dependence on the parameter Δ defined in Eq. (15).

To get the correct scaling for the abscissa, the parameter $\Delta(v_L,m_0,\chi,\tau_W)$ has to be calculated according to Eq. (15). While v_L is a free parameter, the magnetization, the susceptibility, and the free energy of the Wulff droplet per unit volume must be obtained analytically or by other means, e.g., as results of simulations. For the free energy of the

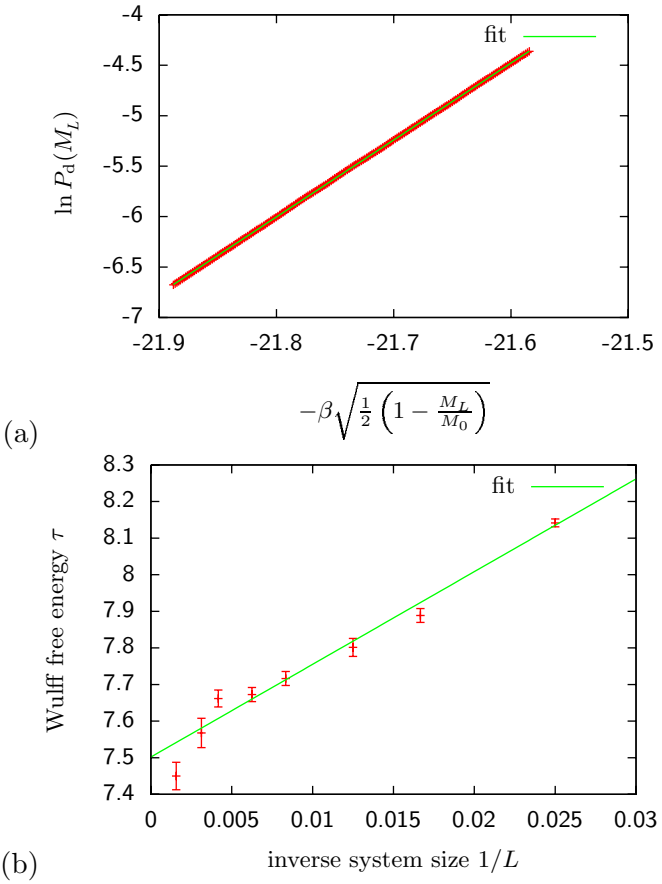

FIG. 7. (Color online) (a) Fit of the distribution $\ln P_d(M_L) = -\beta\tau_W\sqrt{1/2(1-M_L/M_0)}$ for a $V=160\times160$ NNN Ising model at the temperature $T=4.0$ in the range $m=[0.4, 0.4+400/160^2]$. (b) Fit of the Wulff free energy τ_W vs the inverse system size L at temperature $T=4.0$ for $L=40, 80, \ldots, 640$. The error bars are obtained from (at least) ten independent simulations per data point.

Wulff droplet, the analytic expression $\Sigma_W = 2\sqrt{W\Sigma}$ (e.g., Refs. [19,20]) can be used. Here, Σ is the volume of the droplet and W is the volume bounded by the Wulff plot. Putting $\Sigma = 1$ gives the interfacial free energy per unit volume

$$\tau_W(\beta) = 2\sqrt{W}. \tag{22}$$

In the following three subsections we discuss for the three studied models the origin of the constants in question. For the standard Ising model with nearest-neighbor couplings on a square lattice and the Ising model on a triangular lattice, all relevant constants are known from literature, either analytically or from quite long series expansions. This is not the case, however, for the NNN Ising model and, therefore, here we had to apply simulations to retrieve the values.

A. Parameters for the NN Ising model on a square lattice

The critical temperature of the Ising model was given in 1941 by Kramers and Wannier [21]. Using self-duality arguments they obtained the expression

$$T_c = \frac{2}{\ln(1+\sqrt{2})}. \tag{23}$$

For the spontaneous magnetization m_0 there exists the famous Onsager-Yang analytical solution [22,23]

$$m_0(\beta) = [1 - \sinh^{-4}(2\beta)]^{1/8}. \tag{24}$$

Also the susceptibility χ is known virtually to arbitrary precision from very long series expansions, e.g., Orrick *et al.* [24] give the formula

$$\chi(\beta) = \beta\sum_{i=0}^{n} c_i u^{2i} \quad \text{with} \quad u = \frac{1}{2\sinh(2\beta)} \tag{25}$$

and

$$c = \{0,0,4,16,104,416,2\,224,8\,896,43\,840,175\,296,$$
$$825\,648,3\,300\,480,15\,101\,920,\ldots\}$$

up to order 323 (at $T=1.5$ the last term contributes $\approx 0.28\times10^{-158}$). The volume of the Wulff plot is given by [20]

$$W = \frac{4}{\beta^2}\int_0^{\beta\sigma_0} dx\, \cosh^{-1}\left(\frac{\cosh^2(2\beta)}{\sinh(2\beta)} - \cosh(x)\right), \tag{26}$$

where

$$\sigma_0 = 2 + \frac{1}{\beta}\ln[\tanh(\beta)] \tag{27}$$

is the interface tension of the (1,0) surface (i.e., in direction of the axis). For the (1,1) surface the exact expressions reads [25,26]

$$\sigma_1 = \frac{\sqrt{2}}{\beta}\ln[\sinh(2\beta)]. \tag{28}$$

B. Parameters for the NN Ising model on a triangular lattice

The critical temperature for the triangular lattice is [27]

$$T_c = \frac{4}{\ln 3}. \tag{29}$$

For the spontaneous magnetization Potts [28] gave in 1952 the expression

$$m_0(\beta) = \sqrt{1 - \frac{16\exp(-12\beta)}{[1-\exp(-4\beta)][1+3\exp(-4\beta)]}}. \tag{30}$$

In contrast to the large number of low-temperature series expansions for the susceptibility of the square lattice, we are aware of only two published papers for the triangular lattice [29,30]. In the second paper two more coefficients for the same series are given:

$$\chi(\beta) = \beta\sum_{i=1}^{n} c_i u^i \quad \text{with} \quad u = \exp(-4\beta), \tag{31}$$

where

$$c = \{0,0,4,0,48,16,516,288,5\ 328,3\ 840,53\ 676,$$
$$45\ 488,531\ 600,505\ 584,5\ 199\ 404,$$
$$5\ 399\ 136,50\ 369\ 760,56\ 095\ 776,$$
$$484\ 296\ 732,571\ 273\ 344,4\ 628\ 107\ 216\}.$$

Finally, for the volume of the Wulff plot no explicit solution is available. Shneidman and Zia [31] showed the correct solution to be the integral

$$W(\beta) = 6\int_0^{\pi/6} d\theta\, r^2(\theta) \tag{32}$$

with a function $r(\theta)$ given implicitly by

$$\frac{3+\exp(2\beta)}{-2+2\exp(2\beta)} = \cosh\left[r\beta\sin\left(\frac{\pi}{3}-\theta\right)\right] + \cosh[r\beta\sin(\theta)] + \cosh\left[r\beta\sin\left(\frac{\pi}{3}+\theta\right)\right]. \tag{33}$$

For the angles $\theta_l = l\pi/6$, $l=0,1,\ldots,11$, the interface tension in the direction normal to the equilibrium surface is given by $r(\theta_l)$. In the direction $\theta=\pi/6$ the minimal radius $r_{\min}$ can be found to have the value

$$r_{\min} = \sigma_0 = \frac{2}{\beta}\cosh^{-1}\left(\frac{1-e^{4\beta}+e^{2\beta}\sqrt{e^{8\beta}-2e^{4\beta}-3}}{2e^{4\beta}-2}\right). \tag{34}$$

The maximal radius $r_{\max}$ is located at $\theta=0$ and Eq. (33) simplifies greatly to

$$r_{\max} = \sigma_1 = \frac{2}{\sqrt{3}\beta}\ln\left(\frac{e^{4\beta}-1}{2}\right). \tag{35}$$

C. Parameters for the NNN Ising model on a square lattice

For the next-nearest-neighbor model none of our parameters are known exactly. The inverse critical temperature was given by Nightingale and Blöte [32] using a transfer-matrix technique they call "phenomenological renormalization" to be

$$\beta_c = 0.190\ 192\ 69(5). \tag{36}$$

In [33] this value was independently established using Monte Carlo simulations and finite-size scaling procedures. All other quantities are unknown in the literature and, therefore, computer simulations must provide the values. In the case of the magnetization and the magnetic susceptibility this is quite easy. A simple Monte Carlo algorithm at the desired temperature gives a time series of the magnetization M. Then the spontaneous magnetization and the susceptibility are given by

$$m_0 = \frac{1}{VN}\sum_{i=1}^{N} M_i \tag{37}$$

and

$$\chi = \frac{\beta}{V}\left[\frac{1}{N}\sum_{i=1}^{N} M_i^2 - \left(\frac{1}{N}\sum_{i=1}^{N} M_i\right)^2\right], \tag{38}$$

where N is the number of Monte Carlo measurements and $V=L\times L$ the volume of the system. In the desired temperature range $T\approx(2/3)T_c$ the spatial correlation length ξ is very small, and therefore already for moderate lattice sizes rather precise estimates can be achieved.[4] Figure 6 shows the results of a Metropolis simulation of the NNN Ising model at $T=4.0$.

To obtain the Wulff free energy is a much more demanding task. Several methods are known, e.g., thermodynamic integration [34,35]. Here, we will discuss two different ideas, namely, a fit to the distribution of $P(M)$ and a simple argument that the value of τ_W does not differ much from the appropriately scaled planar surface tension σ_0.

For our first method, we exploit the fact that the probability distribution for a droplet of volume v_d can be written as [36]

$$P_d \propto \exp(-\beta\tau_W\sqrt{v_d}). \tag{39}$$

Using Eq. (2) and under the assumption $v_d \approx v_L$ the free energy in the exponent is

$$F_d = \tau_W\sqrt{v_d} \approx \tau_W\sqrt{\frac{1}{2}\left(1-\frac{M_L}{M_0}\right)}. \tag{40}$$

The assumption that the total overturned volume v_L is consumed by the droplet volume v_d is certainly satisfied the better the larger the droplet is. As is well known, the droplet can grow until it reaches the so-called droplet-strip transition point, which is roughly located at

$$M_{\rm ds} = M_0\left(1-\frac{2}{\pi}\right). \tag{41}$$

With Eqs. (39) and (40), a linear fit of the form $y=\tau_W x+c$ can be achieved, where $y=\ln P_d$ and $x=-\beta\sqrt{(1/2)(1-M_L/M_0)}$. Figure 7(a) shows such a fit for the 160×160 NNN Ising model at the temperature $T=4.0$ and for a range $m=[0.4000,0.4156]$, which is close to the droplet-strip transition point located at $m_{\rm ds}=m_0(1-2/\pi)\approx0.3442$. The data stem from a constrained multimagnetic simulation. To extract the value of the Wulff free energy in the thermodynamic limit of large systems, several simulations at different lattice sizes must be performed. In Fig. 7(b) the scaling of the Wulff free energy is shown in dependence on the inverse lattice size. The intersection of the linear fit with the ordinate gives an estimate of $\tau_W=7.50\pm0.02$.

Finally, we want to make three remarks about the given method. First, we are fully aware of the fact that Eqs. (21) and (9) give a "correction" to the fit done last. Using $v_d(\lambda)$, the fit would be valid for any droplet size up to the condensation-evaporation point and not only for large drop-

[4] For too small lattice sizes, the system can "tunnel" from one peak of the magnetization, e.g., at $m=m_0$, to the peak of opposite magnetization $m=-m_0$, or vice versa. To be on the safe side, we checked the time series for this behavior.

lets near the droplet-strip transition point. But, on the other hand, the fit would no longer be linear, and, more important, the theoretical predictions that we want to compare with would be mixed up with the parameter estimation. Second, it is possible to measure during the simulation the droplet size v_d and fit $\tau_W\sqrt{v_d}$ directly, instead of $P(m)$. Here, the disadvantage lies in the computational effort to measure the droplet size. While the magnetization comes at no additional cost, a single measurement of the volume of the largest droplet needs $O(V)$ operations. Third, we want to emphasize the importance of the initial starting conditions of the simulation. An ordered start where the first n spins point in one direction and the next $V-n$ in the other direction is in fact a strip configuration. As discussed in Refs. [6,20], between the strip configuration and the droplet configuration there is an exponentially large barrier that might not be overcome during the equilibration phase, even though a droplet configuration has a much lower free energy for the constrained magnetization range chosen.

The second method to obtain τ_W is based on the assumption that, at the considered temperature, the interface tension for different angles θ is roughly isotropic. This can be verified in detail for the NN Ising model, where the interface tension for an arbitrary angle θ is known analytically [37]. For the planar interface the expression (also given by Onsager [27,38,39]) is $\sigma_0^{\mathrm{sq}}=2J+T\ln[\tanh(J/T)]$ and the expression for the "worst case," i.e., along the main diagonal of the lattice, is $\sigma_1^{\mathrm{sq}}=\sqrt{2}T\ln\sinh(2J/T)$ (also given by Fisher and Ferdinand [25]). For all temperatures larger than $T=1.5$, the relative difference of σ_0^{sq} and σ_1^{sq} is smaller than 1.3%. Obviously, the Wulff shape is still rather circular at low temperatures and the squarelike shape becomes apparent only close to $T=0$. With this crude heuristics, the interface tension per unit volume at $T=1.5$ is $2\sqrt{\pi}\sigma_0^{\mathrm{sq}}=4.219$. This is quite close (99.37%) to the correct value $\tau_W^{\mathrm{sq}}=4.245$. An even better approximation is $2\sqrt{\pi}(\sigma_0^{\mathrm{sq}}+\sigma_1^{\mathrm{sq}})/2$, which deviates only 0.006% from the actual value. The same holds true for the triangular lattice. Using Eq. (34) one finds at $T=2.4\approx\frac{2}{3}T_c$ a value of $2\sqrt{\pi}\sigma_0^{\mathrm{tri}}=7.506\,57$, which is only 0.005% smaller than the exact value of τ_W^{tri}. Inclusion of Eq. (35) for the improved estimation $2\sqrt{\pi}(\sigma_0^{\mathrm{tri}}+\sigma_1^{\mathrm{tri}})/2$ yields a remarkably small difference of 6×10^{-7}% from the exact result. A more detailed discussion concerning the approximation of $\sigma(\theta)$ can be found in [31]. For the NNN Ising droplet, the low-temperature Wulff shape is an octagon, i.e., it is much closer to the high-temperature (low-interface-tension) form, namely, a circle. Therefore, it is reasonable to assume that the above approximation might work as well. The planar interface tension can be measured using a multimagnetic simulation (flat in the distribution of the magnetization), the result of which is a double-peaked magnetization density $P(m)$. In the limit of large system sizes L, we have in two dimensions [40]

$$\ln\left(\frac{P_{\mathrm{max}}^{(L)}}{P_{\mathrm{min}}^{(L)}}\right)=2\beta\sigma_0 L, \tag{42}$$

where $P_{\mathrm{min}}^{(L)}$ is the value of the density in the mixed phase region $m\approx0$ and $P_{\mathrm{max}}^{(L)}$ the value at its maxima ($m=\pm m_0$).

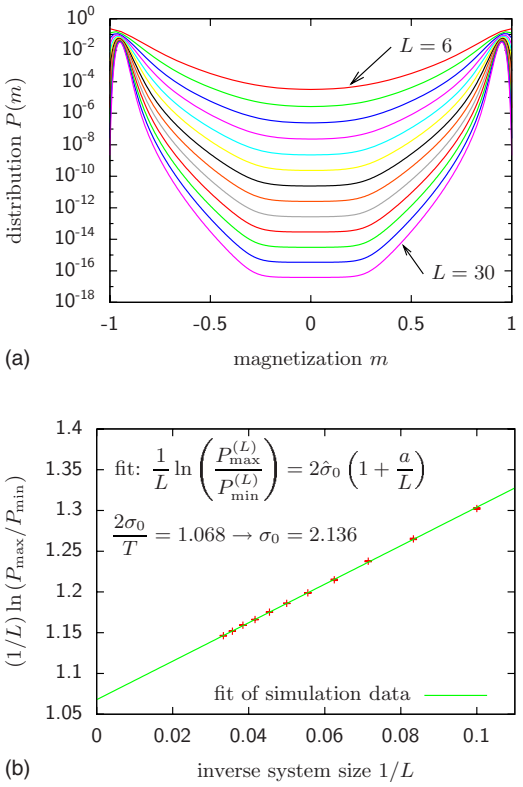

FIG. 8. (Color online) (a) Distribution of the magnetization m for the NNN Ising model at $T=4.0$ and system sizes $L=6,8,\ldots,30$. (b) Scaling of the interface-tension estimates from the histogram method: The straight line shows the fit $\ln(P_{\mathrm{max}}^{(L)}/P_{\mathrm{min}}^{(L)})/L=2\beta\sigma_0(1+a/L)$ for $L\geq10$ with goodness-of-fit parameter χ^2 per degree of freedom of 1.1, yielding a planar interface-tension estimate of $\sigma_0=2.136\pm0.001$.

Figure 8(a) shows the result of 13 multimagnetic simulations for the system sizes $L=6$–30 [33]. For every system the maximum and minimum probabilities $P_{\mathrm{max}}^{(L)}$ and $P_{\mathrm{min}}^{(L)}$ were read off, and by repeating the simulations ten times error bars were obtained. For $L\geq10$ the resulting values are plotted in Fig. 8(b). An infinite-system-size extrapolation in $1/L$ yields a value of $\sigma_0=2.136\pm0.001$ for the planar interface tension. Then the estimate for the Wulff free energy (assuming a circular droplet shape) is $\tau_W\approx2\sqrt{\pi}\times2.136=7.571\pm0.004$, which in fact is a lower bound, as the interface tension is minimal along the directions of the interactions.

Table I gives the numerical values for the spontaneous magnetization m_0, the susceptibility χ, and the Wulff free energy at the temperature T where the simulation took place. The temperature was chosen to be $T\approx0.66T_c-0.76T_c$ which is a good compromise between simulation speed (freezing at low temperatures) and compactness of the droplet (see the right-hand side of Fig. 3 for a typical configuration).

D. Correction of the units in the parameter Δ

After all constants are known, there are still some considerations to be made, before the parameter Δ can be calculated. The magnetization m_0 and the susceptibility χ are in-

TABLE I. Numerical values for the magnetization m_0, susceptibility χ, and Wulff interfacial free energy density τ_W entering the parameter $\Delta=\Delta(v_L,m_0,\chi,\tau_W)$ defined in Eqs. (24)–(37) at the simulation temperature T for the three models studied.

Parameter	NN square	NN triangular	NNN square
T_c	2.269	3.641	5.258
T	1.500	2.400	4.000
T/T_c	0.6610	0.6592	0.7608[a]
m_0	0.9865	0.9829	0.9473
χ	0.02708	0.01959	0.04467
τ_W	4.245	7.507	7.502
$2m_0^2/\tau_W\chi$	16.93	13.14	5.307

[a]The temperature $T=4.0$ was chosen without knowledge of the critical temperature; certainly a value of $T=3.5$ would have been more appropriate.

tensive quantities that follow from the corresponding extensive quantities normalized (divided) by the volume. It is convention that for spin systems the volume is expressed by the number of spins, i.e., every spin accounts for a unit volume. In contrast, the free energy of the Wulff droplet is measured (again by convention) in units of the cell volume, which is calculated given the lattice spacing a as input. A possible way to treat this situation is to normalize all quantities to the cell volume, which would mean that m_0 and χ are given in very unfamiliar units. We refrain from this step in order to keep our results comparable to those in the literature and instead modify Eq. (15) in a very slight way. In order to do so, we define a scaling parameter Δ_{lit} where all parameters are consistent with the conventions from the literature,

$$\Delta_{\text{lit}} = 2\frac{m_0^2}{\chi\tau_W}\frac{v_L^{3/2}}{L^2}. \tag{43}$$

Here, v_L is the *number* of spins of the largest droplet including overturned spins, L^2 is the *total number* of spins of the system, and m_0 and χ are the magnetization and susceptibility normalized to the *total number of spins*. The normalization of the Wulff free energy τ_W does not change as it is given in terms of the unit volume in the literature. Second, we define Δ_{uv} where all quantities are given in terms of the unit volume, which is the meaning intended by Biskup *et al.*,

$$\Delta_{\text{uv}} = 2\frac{\mu_0^2}{X\tau_W}\frac{\Omega^{3/2}}{V}. \tag{44}$$

In this representation, Ω is the *volume* of the largest droplet, V the *volume* of the total system, and μ_0 and X are the magnetization and susceptibility normalized to the *volume* of the total system. If v_0 is the Voronoi volume of one spin [41] (the volume of the Wigner-Seitz cell of one spin) measured in units compatible with τ_W, then we have

$$\Omega = v_L v_0, \tag{45}$$

$$V = L^2 v_0, \tag{46}$$

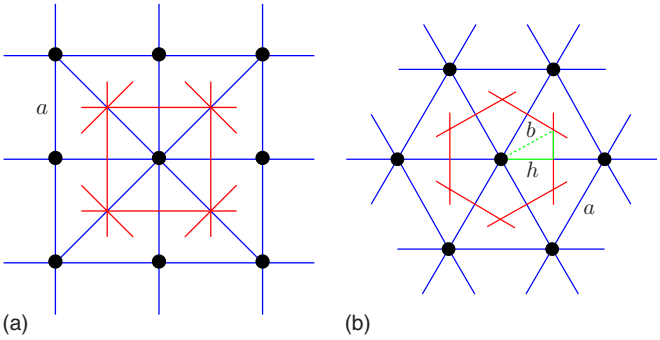

FIG. 9. (Color online) Wigner-Seitz cell of the (a) NNN and (b) triangular lattice. It contains only one lattice site and all points within the cell are closer to this point than to any other lattice site. The red lines indicate the construction principle using the normals to the connection of a lattice to its neighbors.

$$\mu_0 = \frac{M}{V} = \frac{M}{v_0 L^2} = \frac{m_0}{v_0}, \tag{47}$$

$$X = \beta V(\langle\mu^2\rangle - \langle\mu\rangle^2) \tag{48}$$

$$= \beta L^2 v_0\left(\left\langle\frac{m_0^2}{v_0^2}\right\rangle - \left\langle\frac{m_0}{v_0}\right\rangle^2\right) \tag{49}$$

$$= \frac{\beta L^2}{v_0}(\langle m_0^2\rangle - \langle m_0\rangle^2) = \frac{\chi}{v_0}. \tag{50}$$

Now, a geometric "correction factor" α from Δ_{lit} to Δ_{uv} can be defined as

$$\Delta_{\text{uv}} = \alpha\Delta_{\text{lit}}. \tag{51}$$

Using Eqs. (43)–(51), α can be expressed as

$$\alpha = \frac{\Delta_{\text{uv}}}{\Delta_{\text{lit}}} = \frac{2\frac{\mu_0^2}{X\tau_W}\frac{\Omega^{3/2}}{V}}{2\frac{m_0^2}{\chi\tau_W}\frac{v_L^{3/2}}{L^2}} = \frac{1}{\sqrt{v_0}}. \tag{52}$$

To conclude, using the parameters from the literature as given in Table I, the abscissa must not be scaled by Δ but rather by $\Delta/\sqrt{v_0}$, where v_0 is the Voronoi volume of one cell.

For the square lattice, the Voronoi volume that a spin occupies is 1×1, which makes the correction factor transparent. The same holds for the NNN lattice that has (by coincidence) the same geometry as the NN lattice (see Fig. 9). In the case of the triangular lattice, the Voronoi cell is a hexagon. Figure 9(b) displays the situation. If h denotes one-half of the lattice side length a, then it holds that $a=2h$. Every hexagon is made up of six small equilateral triangles of side length b (dotted line). The height of such a triangle is h, given by $h=b\sqrt{3}/2$. It follows that $b=a/\sqrt{3}$. Now, the volume of a hexagon is given by

$$v_0^{\text{hex}} = \frac{3\sqrt{3}}{2}b^2 = \frac{3\sqrt{3}}{2}\left(\frac{a}{\sqrt{3}}\right)^2 = \frac{\sqrt{3}}{2}a^2. \tag{53}$$

Finally, for $a=1$, the geometric factor α for the triangular lattice is

$$\alpha_{\mathrm{tri}} = \frac{1}{\sqrt{v_0}} = \sqrt{\frac{2}{\sqrt{3}}} \approx 1.075\ldots. \tag{54}$$

E. Droplet measurement

As mentioned at the beginning of Sec. III, one of our primary goals was the determination of the volume of the largest droplet. A possible advance would be to set up a multimagnetic simulation and measure the droplet volume every sweep or so. While this is certainly possible, it is not advisable, as the determination of the multimagnetic weight factors $W(m) \approx 1/P(m)$ alone is a demanding task, and in the following analysis there is no use for them. Instead, we arranged several simulations at fixed magnetization m (micromagnetic). Inserting Eq. (3) in (15) and solving for M_L gives the relation between the parameter Δ and the magnetization M_L,

$$M_L(\Delta) = Vm_0 - \left(\frac{2\Delta\chi\tau_W V}{\sqrt{2m_0}}\right)^{2/3}. \tag{55}$$

Solving Eq. (55) for Δ yields

$$\Delta(M_L) = \frac{\sqrt{2m_0}}{2\chi\tau_W V}(Vm_0 - M_L)^{3/2}, \tag{56}$$

which shows that a fixed magnetization results in a fixed value $\Delta(M_L)$. Therefore, we actually selected for every lattice 38 reasonable values $\tilde{\Delta}_i = \{0.00, 0.10, \ldots, 16\}$, with an emphasis on the vicinity of Δ_c. By insertion of $\Delta = \tilde{\Delta}_i$ into (55), a set of corresponding magnetization values M_i (usually noninteger values) was obtained. A subsequent rounding to the next allowed integer value of the magnetization ($\Delta M = \pm 2$) gave the final values for the simulation. To take the influence of the rounding into account, Eq. (56) was used, resulting in the final set of slightly shifted ($\propto 1/\sqrt{V} = 1/L$) Δ_i values that correspond to the integer-valued magnetizations. Finally, v_L was computed using (16), $v_L = \frac{1}{2}(V - M_L/m_0)$, which in general gives a noninteger value. It should be emphasized that in Eqs. (55) and (56) we use for m_0, χ, and τ_W the thermodynamic values, which are strictly valid only in the limit of infinite system size, but as we are mainly interested in the leading scaling behavior of our results, the error introduced here can be neglected.

To enforce the constraint of constant magnetization, we use a Kawasaki update scheme where an up spin is exchanged with a down spin. Since the total number of up and down spins does not change, the magnetization keeps its value as well. This type of nonlocal Monte Carlo move can be accelerated using a table storing the spins sorted according to their direction. Here, one sweep accounts for V spin exchange attempts.

After every sweep our simulation determines the volume of the second-largest cluster which is (by definition) the volume v_d of the droplet. This is done in two steps. First a Hoshen-Kopelman [42] algorithm performs a complete cluster decomposition. Thereby spins connected by NN (or NNN) interactions and pointing in the same direction are assigned a unique number. Figure 10 shows the situation for a spin configuration with NN interactions. The largest (partially drawn) cluster (red) having cluster index 1 is the background; the cluster in the center (green) with cluster index 2 is the droplet we are looking for. Inside this droplet are smaller clusters located with cluster indices 3, 4, and 5 (light blue, yellow, and purple). In the next step a flood-fill routine [43], essentially a geometric depth first search, scans the droplet. Starting from an arbitrary position (which was recorded during the cluster identification step), it stops only when it finds spins that belong to the largest cluster (background). Thereby spins and clusters of opposite sign that lie within the droplet are subsumed. The result of this operation is shown in Fig. 10(b). The thick blue line indicates the border between the droplet, i.e., cluster number 2, and all clusters that do not have the cluster number of the background, and the background. While this method is easy to implement for NN interactions, in the case of the NNN square lattice there are some pathological cases. Figure 11 shows such an

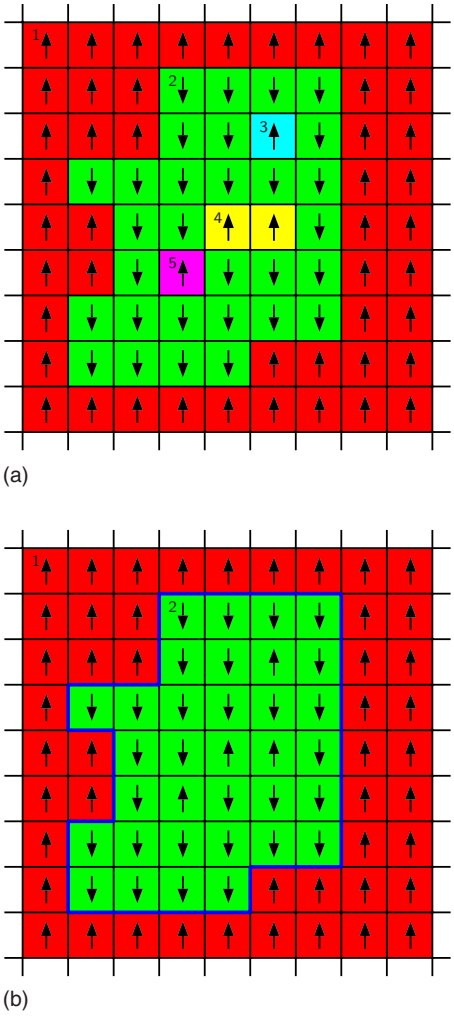

FIG. 10. (Color online) Cutout of a spin configuration; the red background cluster should be much larger [cf. right-hand side (RHS) of Fig. 3]. (a) The colors and the (small) numbers indicate the clusters detected and enumerated by the Hoshen-Kopelman routine. (b) The thick blue line surrounds the droplet (second largest cluster) found by the flood-fill routine.

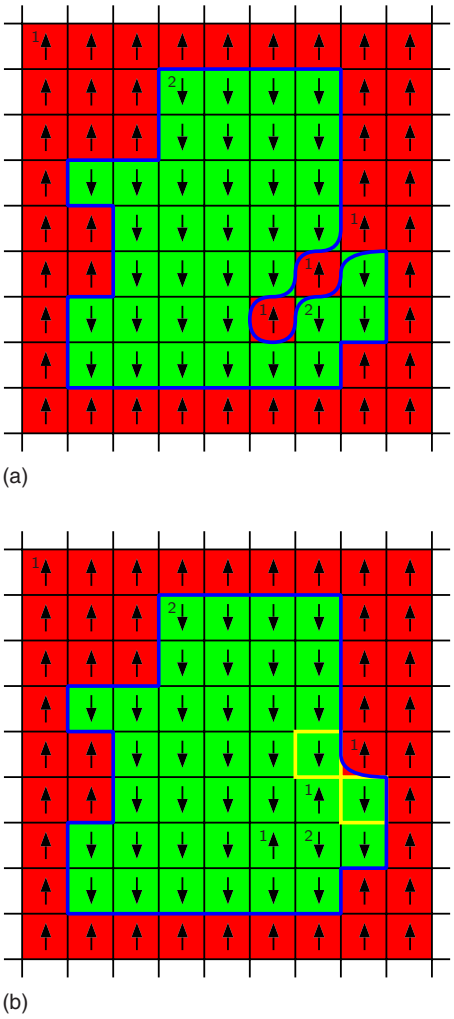

FIG. 11. (Color online) (a) Cutout of a spin configuration for the NNN Ising model with a droplet (green) detected by the flood-fill algorithm. Apparently, the inclusion on the lower right side of the droplet (two spins) has a connection to the background and does not count toward the volume of the droplet. (b) Another way to interpret the situation where the spins are part of the droplet.

ambiguous situation. Figure 11(a) presents the droplet as identified by our algorithm. In contrast, Fig. 11(b) is an (imaginary) alternative version resulting from the closing of the inclusion of background spins. The justification of the right pictures is given by the fact that the NNN model has an interaction along the diagonal which connects the two surface spins (yellow). Fortunately, it is not necessary to decide which scenario is the more physical one. Every inclusion of reasonable size causes a large number of broken bonds at its surface. Therefore, configurations with inclusions are highly suppressed for temperatures well below the Curie point. To be on the safe side, we analyzed several simulations of the NNN square lattice for different system sizes with both methods at the same time, i.e., for identical configurations the droplet was measured a second time with an algorithm that closes inclusions, and we found negligible differences. In the end we decided to keep things as simple as possible and therefore used only the combination Hoshen-Kopelman–flood-fill method for our data generation.

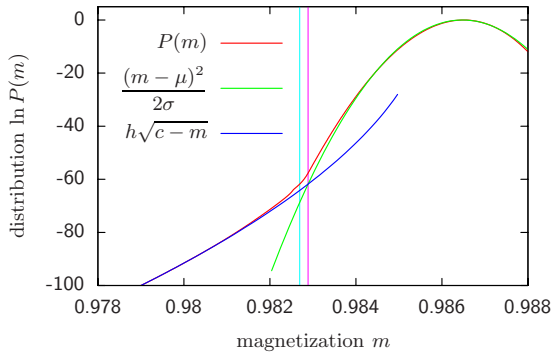

FIG. 12. (Color online) Gaussian fit and stretched exponential fit of the distribution of the magnetization $P(m)$ for the result of an $L=640$ NN Ising simulation at $T=1.5$. The left vertical line (magenta) indicates the transition magnetization $M_L(\Delta_c)/V$ predicted by Eq. (55), while the right vertical line (purple) coincides with the intersection point of the two fits.

IV. NUMERICAL RESULTS

For all three systems and at every value of Δ we performed simulations at five different lattices sizes $L=40$, 80, 160, 320, and 640. Every simulation ran at least 20 000 sweeps for the thermalization and at least 200 000 sweeps for the measurements. To obtain the error bars reliably, ten independent simulations were run for each data point. For the creation of pseudorandom numbers we use the R250/521 generator [44,45].

Having the numerical values of m_0, χ, and τ_W in place (see Sec. III), the region of interest can be estimated. For $\Delta=0.92\approx\Delta_c$ and the values from Table I corresponding to the NN Ising model, for $L=640$ the magnetization is estimated with Eq. (55) to be $m\approx0.9827$. To see the relevance of this figure we performed a multimagnetic simulation coupled with the parallel tempering algorithm [46] for the NN Ising model, the result of which can be seen in Fig. 2. It shows the upper part (in the vicinity of the magnetization peak in Fig. 1) of the distribution of the magnetization $P(m)$, which for larger lattice sizes exhibits a clear cusp that divides the evaporated and condensed regions. Within the evaporated region it has a Gaussian form according to Eq. (7), while in the condensed region a stretched exponential behavior is visible; cf. Eq. (4). To verify this quantitatively, Fig. 12 shows a fit of a Gaussian curve and a stretched exponential curve to the upper part of the distribution of the magnetization $\ln P(m)$ for the NN Ising model. The point of intersection $m_\times$ is given by the condition

$$h\sqrt{c-m_\times}+d=-\frac{(m_\times-m_{\max})^2}{2\sigma^2}, \tag{57}$$

the solution of which is a fourth-order equation. With the parameters from the fit $m_{\max}=0.9864$, $\sigma^2=1.042\times10^{-7}$, $c=0.9858$, and $h=-1340$, it evaluates to $m_\times=0.9829$, which is quite close to the aforementioned value calculated with Eq. (55). The Gaussian fit which corresponds to the pure fluctuation part where $\lambda=0$ can be compared to $-\beta F_f$ from Eq. (7). It yields for the susceptibility $\chi=\beta V\sigma^2=0.6666\times640^2\times1.042\times10^{-7}\approx0.028$, a value quite close to the infinite-

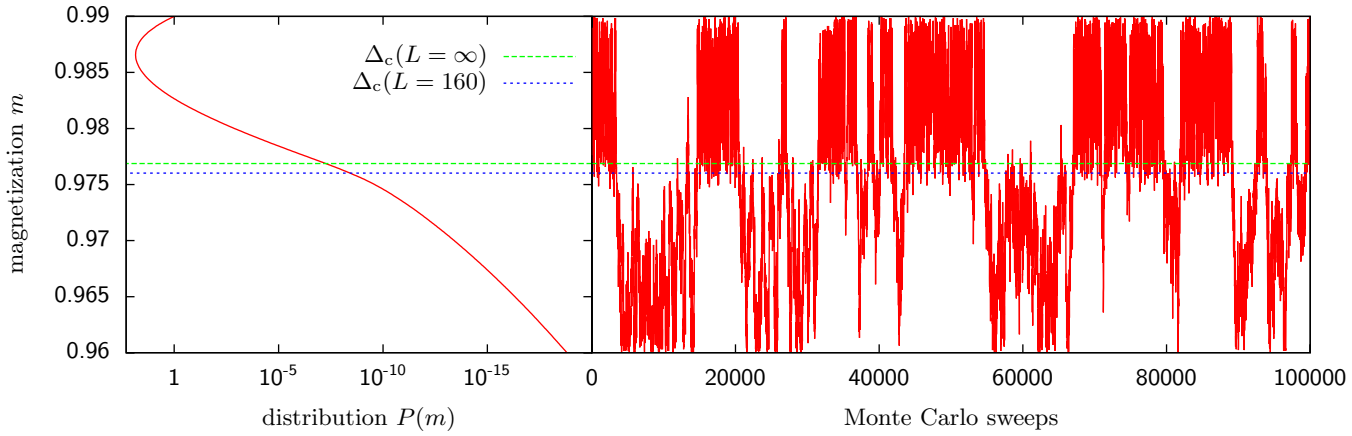

FIG. 13. (Color online) Time series of the magnetization of an $L=160$ NN Ising simulation at temperature $T=1.5$. The distribution on the LHS corresponds to the times series on the RHS and both were measured during the same simulation run. The lower (green) and upper (blue) horizontal lines indicate the transition magnetization calculated from Eq. (55) for lattice sizes $L=160$ and $L\to\infty$, respectively. The blocks in the time series are a typical sign of a barrier in the free energy.

volume value given in Table I of 0.027 08. In the droplet-dominated regime we have approximated the full mixed phase expression by neglecting the contributions of the fluctuations, which corresponds to putting $\lambda=1$ in Eq. (12). Over the fit range the neglected part contributes less than 4%. Even in the worst case, located at the cusp where $\lambda=2/3$, it amounts only to a value of approximately 9%. To obtain these values the ratio $F_d(1)/F(\lambda)=4\sqrt{\lambda}/(3\lambda+1)$ is evaluated using Eq. (21) in conjunction with Eq. (56), which yields an expression $\lambda=\lambda(M_L)$. This is corroborated by the fact that, when the droplet regime is fitted without fluctuations, from $-\beta F_d(1)$ the Wulff free energy is approximated as $\tau_W=-h/[\beta\sqrt{V/(2c)}]=1340/[0.6666\times\sqrt{640^2/(2\times0.9858)}]\approx4.410$, which is, again, quite close to the value of 4.245 given in Table I.

To have another "visual proof" that something different is happening on the two sides of the cusp in Fig. 2, we took several snapshots of the configurations that occurred during a simulation run. The two plots of Fig. 3 display an evaporated (left) and a condensed system (right), respectively. Both systems have the same number of overturned spins, i.e., the same magnetization, which was chosen to be right at the transition point. While both configurations occurred during an actual simulation run, they do present extreme cases. When the set of the largest cluster sizes recorded in the simulation run is considered, the evaporated cluster configuration corresponds to the smallest number in the set and the condensed configuration corresponds to the largest number in the set.

A final affirmation that the point under consideration was chosen correctly can be derived from a look at the time series of the magnetization m in Fig. 13. The direct comparison shows a block structure in the time series that coincides with the cusp in the distribution $P(m)$. Clearly, this is a sign of a barrier in the free energy.

In Figs. 14–16 we show our main results, the fraction $\lambda(\Delta)$ for the three observed lattices. The (black) solid line is the analytical value of λ as shown in Fig. 5. Clearly, for larger lattice sizes the theoretical value is approached by the results of the simulation. Figure 14(a) shows λ in dependence on the magnetization m. In Fig. 14(b) λ is plotted for the same set of data points, but this time in dependence on Δ, which essentially is a rescaling with $v_L^{3/2}$. While in Fig. 14(a) the important region is barely visible, the rescaling leads to a

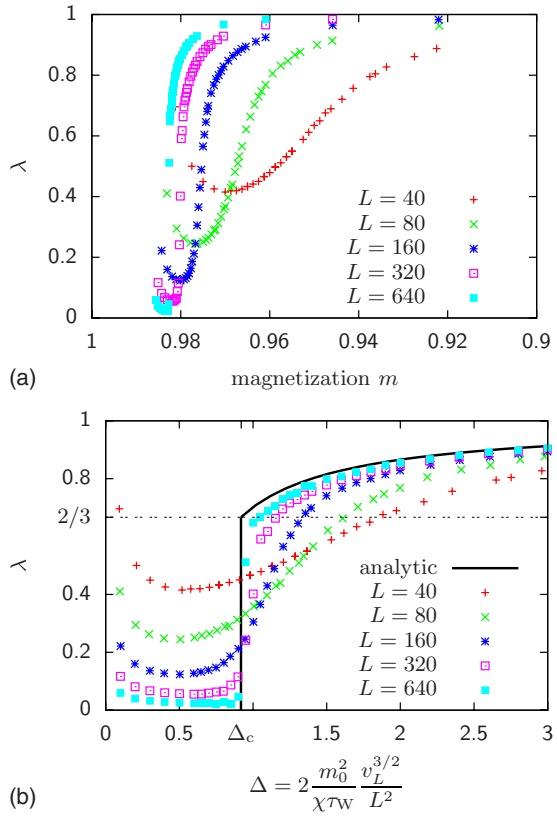

FIG. 14. (Color online) Fraction λ for the 2D NN Ising model on square lattices of size $L=40,80,\ldots,640$ with periodic boundary conditions at the temperature $T=1.5\approx0.66T_c$. The error bars are not plotted since their size is much smaller than that of the data symbols. To show the influence of the scaling of the abscissa, (a) and (b) use the same data. While in (a) the fraction λ is given in units of the magnetization in (b) it is given in units of Δ. The solid line in (b) shows the analytical solution in the limit $L\to\infty$.

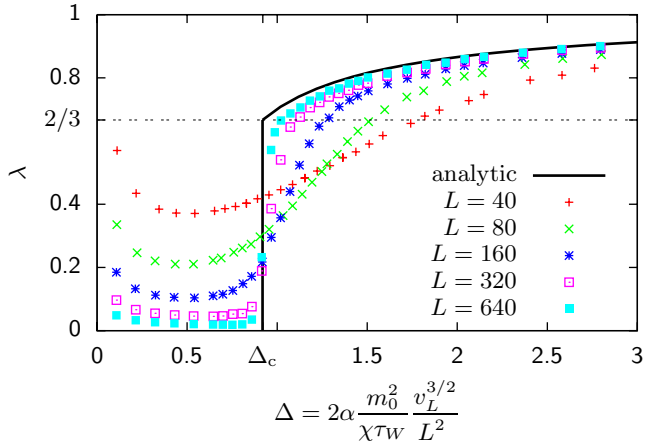

FIG. 15. (Color online) Fraction λ for the triangular Ising model on square lattices of size $L=40,80,\ldots,640$ with periodic boundary conditions at the temperature $T=2.4\approx 0.66T_c$. Here, $\alpha=1/\sqrt{v_0}=\sqrt{2/\sqrt{3}}\approx 1.075\ldots$ is the geometric factor, defined in Sec. III D. The error bars are not plotted since their size is much smaller than that of the data symbols. The solid line shows the analytical solution in the limit $L\to\infty$.

blowup of the transition region, making the theoretically predicted jump from $\lambda_\Delta\approx 0$ to $\lambda_\Delta\approx 2/3$ at $\Delta_c\approx 0.92$ observable. This confirms that at the evaporation-condensation transition only 2/3 of the excess of the magnetization goes into the droplet, while the rest remains in the background fluctuations. The increase of λ_Δ for $\Delta\to 0$ can be explained by the fact that the minimal cluster size is 1 and not an arbitrarily small fraction. In contrast, the excess that can be fixed analytically using Eq. (15) can be much smaller than 1.

In Fig. 17 we compare λ of the three different models for the same system size $L=640$. The nice agreement of the data points is a clear indication of the lattice-independent universal behavior of the theory. An explanation for the slight discrepancy between the NN and the triangular lattice on the one side and the NNN model on the other might be given by the slightly different temperature ratio T/T_c (see Table I).

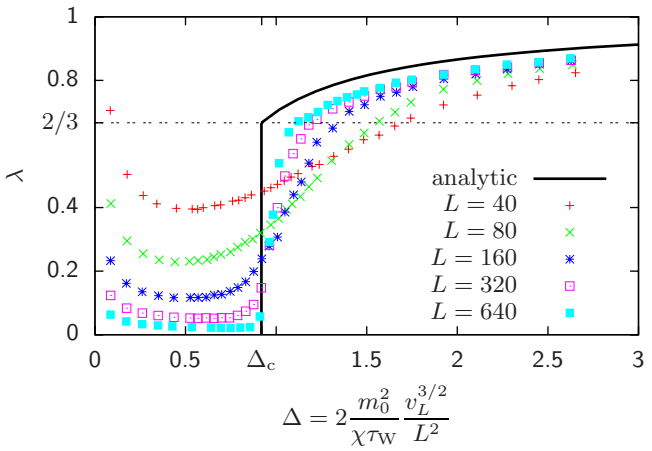

FIG. 16. (Color online) Fraction λ for the 2D NNN Ising model on square lattices of size $L=40,80,\ldots,640$ with periodic boundary conditions at the temperature $T=4.0\approx 0.76T_c$. The error bars are not plotted since their size is much smaller than that of the data symbols. The solid line shows the analytical solution in the limit $L\to\infty$.

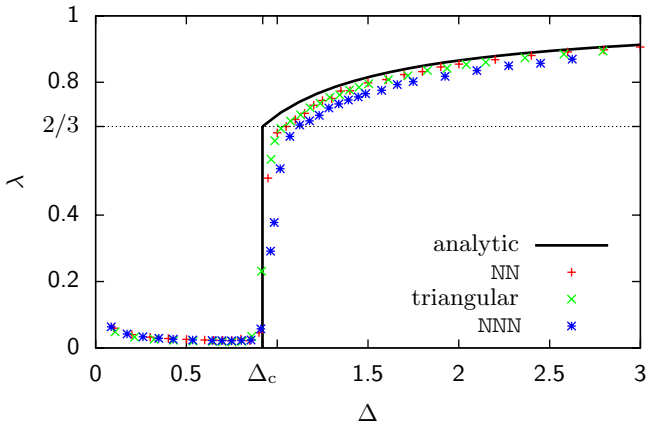

FIG. 17. (Color online) Comparison of the fraction λ for the three observed Ising models (NN, triangular, and NNN) for the size $L=640$ and the temperatures $T=1.5,2.4,4.0$.

Finally, under the assumption that the jump in the droplet size λ from 0 to 2/3 occurs at Δ_c, it is possible to determine one of the constants included in the rescaling factor Δ. Plotting the fraction λ against $v_L^{3/2}/L^2$ for two different L, e.g., $L=320$ and 640, gives us a point of intersection δ. At least for large lattice sizes, this point should approach Δ_c if correctly scaled by a factor $D=2m_0^2/\chi\tau_W$ (respectively, $D=2\alpha m_0^2/\chi\tau_W$ for the triangular lattice), i.e., asymptotically

$$\Delta_c = D\delta \tag{58}$$

holds. When δ is measured, the unknown factor D is given by $D=\Delta_c/\delta$. Certainly, the most interesting quantity from a computational point of view is the interfacial tension τ_W, which can be computed as $\tau_W=2m_0^2/\chi D$ if the spontaneous magnetization m_0 and the susceptibility χ are known. In the case of the NN square lattice, the point of intersection for $L=320$ and 640 is $\delta=0.053\,78$, which gives a scaling factor of $D=17.08$. Consequently, the interface tension is $\tau_W=4.208$, which is less than 1% off from the analytical value given in Table I.

V. CONCLUSION

Our Monte Carlo data clearly confirm the theoretical considerations of Biskup *et al.* [7,8] for the case of the 2D nearest-neighbor Ising system. While their results are valid only in the thermodynamic limit of large systems, we have shown that for practically accessible sizes the theory can also be applied. The observed finite-size scaling behavior fits perfectly with their predictions for the infinite system.

Moreover, we have demonstrated that the theory, which to date has only been proven for the square lattice nearest-neighbor case, is actually universal in the sense that it is independent of the underlying lattice. The Ising model on the 2D triangular lattice and on the 2D next-nearest-neighbor lattice both approach the theoretically expected results nicely. Apparently, for the same relative temperature T/T_c the finite-size behavior is identical.

In order to achieve the correct scaling of the abscissa, we presented several methods to estimate the Wulff free energy τ_W numerically. While in theory it should be straightforward to extract the value from the distribution of the magnetization, due to limitations in the computer time for temperatures near the critical one, it can be more advantageous to resort to the isotropic approximation.

All simulations were performed in thermal equilibrium, and the abundance of droplets of intermediate size could be confirmed visually by looking at the distribution of droplets. We just state this fact here, while a more detailed analysis and the corresponding graphs will be presented later, together with more results on the finite-size scaling behavior of the systems and the shape of the free-energy barrier associated with the evaporation-condensation transition.

ACKNOWLEDGMENTS

We are indebted to Kurt Binder and Thomas Neuhaus for sharing their physical insight into the droplet nucleation mechanism, and wish to thank Roman Kotecký for helpful discussions on the formulation used in the present work. The work was supported by the Deutsche Forschungsgemeinschaft (DFG) under Grants No. JA483/22-1 and No. JA483/23-1 and in part by the EU RTN Network "ENRAGE: Random Geometry and Random Matrices: From Quantum Gravity to Econophysics" under Grant No. MRTN-CT-2004-005616. Supercomputer time at NIC Jülich under Grant No. hlz10 is also gratefully acknowledged.

[1] M. E. Fisher, Rep. Prog. Phys. **30**, 615 (1967).
[2] J. E. Mayer and W. W. Wood, J. Chem. Phys. **42**, 4268 (1965).
[3] K. Binder and M. H. Kalos, J. Stat. Phys. **22**, 363 (1980).
[4] H. Furukawa and K. Binder, Phys. Rev. A **26**, 556 (1982).
[5] K. Kaski, K. Binder, and J. D. Gunton, Phys. Rev. B **29**, 3996 (1984).
[6] T. Neuhaus and J. S. Hager, J. Stat. Phys. **113**, 47 (2003).
[7] M. Biskup, L. Chayes, and R. Kotecký, Europhys. Lett. **60**, 21 (2002).
[8] M. Biskup, L. Chayes, and R. Kotecký, Commun. Math. Phys. **242**, 137 (2003).
[9] K. Binder, Physica A **319**, 99 (2003).
[10] P. Virnau, L. G. MacDowell, M. Müller, and K. Binder, in *Computer Simulation Studies in Condensed Matter Physics XVI*, edited by D. P. Landau, S. M. Lewis, and H.-B. Schüttler (Springer, Berlin, 2004).
[11] L. G. MacDowell, P. Virnau, M. Müller, and K. Binder, J. Chem. Phys. **120**, 5293 (2004).
[12] L. G. MacDowell, V. K. Shen, and J. R. Errington, J. Chem. Phys. **125**, 034705 (2006).
[13] A. Nußbaumer, E. Bittner, T. Neuhaus, and W. Janke, Europhys. Lett. **75**, 716 (2006).
[14] M. Biskup, L. Chayes, and R. Kotecký, J. Stat. Phys. **116**, 175 (2004).
[15] J. Lee, M. A. Novotny, and P. A. Rikvold, Phys. Rev. E **52**, 356 (1995).
[16] M. Pleimling and W. Selke, J. Phys. A **33**, L199 (2000).
[17] M. Pleimling and A. Hüller, J. Stat. Phys. **104**, 971 (2001).
[18] G. Wulff, Z. Kristallogr. Mineral. **34**, 449 (1901).
[19] R. K. P. Zia and J. E. Avron, Phys. Rev. B **25**, 2042 (1982).
[20] K. Leung and R. K. P. Zia, J. Phys. A **23**, 4593 (1990).
[21] H. A. Kramers and G. H. Wannier, Phys. Rev. **60**, 252 (1941).
[22] L. Onsager, Nuovo Cimento, Suppl. **6**, 261 (1949).
[23] C. N. Yang, Phys. Rev. **85**, 808 (1952).
[24] W. P. Orrick, B. G. Nickel, A. J. Guttmann, and J. H. H. Perk, Phys. Rev. Lett. **86**, 4120 (2001).
[25] M. E. Fisher and A. E. Ferdinand, Phys. Rev. Lett. **19**, 169 (1967).
[26] C. Rottman and M. Wortis, Phys. Rev. B **24**, 6274 (1981).
[27] R. J. Baxter, *Exactly Solved Models in Statistical Mechanics* (Academic Press, London, 1982).
[28] R. B. Potts, Phys. Rev. **88**, 352 (1952).
[29] M. F. Sykes, D. S. Gaunt, J. L. Martin, S. R. Mattingly, and J. W. Essam, J. Math. Phys. **14**, 1071 (1973).
[30] M. F. Sykes, M. G. Watts, and D. S. Gaunt, J. Phys. A **8**, 1448 (1975).
[31] V. A. Shneidman and R. K. P. Zia, Phys. Rev. B **63**, 085410 (2001).
[32] M. P. Nightingale and H. W. J. Blöte, J. Phys. A **15**, L33 (1982).
[33] A. Nußbaumer, E. Bittner, and W. Janke, Europhys. Lett. **78**, 16004 (2007).
[34] E. Bürkner and D. Stauffer, Z. Phys. B: Condens. Matter **53**, 241 (1983).
[35] M. Hasenbusch and K. Pinn, Physica A **203**, 189 (1994).
[36] S. B. Shlosman, Commun. Math. Phys. **125**, 81 (1989).
[37] J. E. Avron, H. van Beijeren, L. S. Schulman, and R. K. P. Zia, J. Phys. A **15**, L81 (1982).
[38] L. Onsager, Phys. Rev. **65**, 117 (1944).
[39] B. M. McCoy and T. T. Wu, *The Two-Dimensional Ising Model* (Harvard University Press, Cambridge, MA, 1973).
[40] W. Janke, in *Computer Simulations of Surfaces and Interfaces*, edited by B. Dünweg, D. P. Landau, and A. I. Milchev, NATO Science Series II: Mathematics, Physics, and Chemistry Vol. 114 (Kluwer, Dordrecht, 2003), pp. 111–135.
[41] A. Okabe, B. Boots, K. Sugihara, and S. N. Chius, *Spatial Tessellations: Concepts and Applications of Voronoi Diagrams* (John Wiley & Sons, Chichester, U.K., 1999).
[42] J. Hoshen and R. Kopelman, Phys. Rev. B **14**, 3438 (1976).
[43] M. K. Agoston, *Computer Graphics and Geometric Modelling* (Springer, London, 2004).
[44] A. Heuer, B. Dünweg, and A. M. Ferrenberg, Comput. Phys. Commun. **103**, 1 (1997).
[45] W. Janke, in *Quantum Simulations of Complex Many-Body Systems: From Theory to Algorithms*, edited by J. Grotendorst, D. Marx, and A. Muramatsu, NIC Series Vol. 10 (John von Neumann Institute for Computing, Jülich, 2002), pp. 423–445.
[46] D. J. Earl and M. W. Deem, Phys. Chem. Chem. Phys. **7**, 3910 (2005).